Journal for ImmunoTherapy of Cancer

Intratumoral CD103+ CD8+ T cells predict response to PD-L1 blockade

Romain Banchereau,[1] Avantika S. Chitre,[2] Alexis Scherl,[3] Thomas D. Wu,[4] Namrata S. Patil,[1] Patricia de Almeida,[2,5] Edward E. Kadel, III,[1] Shravan Madireddi,[2] Amelia Au-Yeung,[6] Chikara Takahashi,[6] Ying-Jiun Chen,[7,8] Zora Modrusan,[7] Jacqueline McBride,[6] Rhea Nersesian,[1] Ehab A. El-Gabry,[9] Mark D. Robida,[9] Jeffrey C. Hung,[3] Marcin Kowanetz,[1,10] Wei Zou,[11] Mark McCleland,[1] Patrick Caplazi,[3] Shadi Toghi Eshgi,[6] Hartmut Koeppen,[3] Priti S. Hegde,[12] Ira Mellman,[2] W. Rodney Mathews,[6] Thomas Powles,[13] Sanjeev Mariathasan,[1] Jane Grogan,[2] William E O'Gorman [6]

To cite: Banchereau R, Chitre AS, Scherl A, *et al*. Intratumoral CD103+ CD8+ T cells predict response to PD-L1 blockade. *Journal for ImmunoTherapy of Cancer* 2021;**9**:e002231. doi:10.1136/jitc-2020-002231

► Additional material is published online only. To view, please visit the journal online (http://dx.doi.org/10.1136/jitc-2020-002231).

RB and ASC contributed equally. AS, TDW and NSP contributed equally.
SM, JG and WEO contributed equally.

RB and ASC are joint first authors.

SM, JG and WEO are joint senior authors.

Accepted 02 March 2021

For numbered affiliations see end of article.

Correspondence to
Dr William E O'Gorman; ogormanw@gene.com

Dr Jane Grogan; jane.grogan@gmail.com

Dr Sanjeev Mariathasan; sanj@gene.com

ABSTRACT

Background CD8+ tissue-resident memory T (T_{RM}) cells, marked by CD103 (*ITGAE*) expression, are thought to actively suppress cancer progression, leading to the hypothesis that their presence in tumors may predict response to immunotherapy.

Methods Here, we test this by combining high-dimensional single-cell modalities with bulk tumor transcriptomics from 1868 patients enrolled in lung and bladder cancer clinical trials of atezolizumab (anti-programmed cell death ligand 1 (PD-L1)).

Results *ITGAE* was identified as the most significantly upregulated gene in inflamed tumors. Tumor CD103+ CD8+ T_{RM} cells exhibited a complex phenotype defined by the expression of checkpoint regulators, cytotoxic proteins, and increased clonal expansion.

Conclusions Our analyses indeed demonstrate that the presence of CD103+ CD8+ T_{RM} cells, quantified by tracking intratumoral CD103 expression, can predict treatment outcome, suggesting that patients who respond to PD-1/PD-L1 blockade are those who exhibit an ongoing antitumor T-cell response.

INTRODUCTION

Checkpoint therapies can induce potent and durable clinical responses in subsets of patients with cancer across multiple indications. Treatment regimens targeting programmed cell death 1 (PD-1) or programmed cell death ligand 1 (PD-L1) disrupt an inhibitory signaling program in T cells that reduces their cytolytic activity.[1] Thus, blockade of PD-1/PD-L1 binding has been hypothesized to result in the reinvigoration of these T cells and their subsequent killing of tumor cells. While a subset of patients achieve robust antitumor responses with these therapies, many do not, with minimal response rates of 20%–30% across indications such as melanoma, non-small cell lung, urothelial, head and neck, gastrointestinal, and hepatocellular cancers.[2] As such, the variability in clinical response to checkpoint inhibitors has generated interest in the heterogeneity and function of the intratumoral T cells critical for efficacy.[3] Much attention has been paid to an 'exhausted' population of CD8+ T cells that exhibit multiple checkpoint regulators and are presumed to have diminished effector function due to chronic antigen exposure.[1] However, the relationship between exhaustion and response to checkpoint blockade is controversial. While some studies correlate exhaustion to poor clinical outcomes,[4–9] others have defined a subpopulation of CD103+ CD8+ tissue-resident memory T (T_{RM}) cells that appear exhausted, but are also proliferative and associate with cancer survival.[10]

T_{RM} cells are a specialized population of T cells responsible for the rapid initiation of local immune responses within epithelial tissues, thereby providing protective immunity against invading microbes.[11] T_{RM} cells are broadly distributed in adult human tissues such as the skin, lungs, intestines, and brain.[12 13] Furthermore, T_{RM} cells have been implicated in mediating proinflammatory responses in autoimmune diseases such as psoriasis, alopecia areata, vitiligo, as well as ulcerative colitis.[14 15] T_{RM} cells are defined phenotypically by their expression of CD103 (integrin αE or *ITGAE*), which pairs with integrin β7 to form the αEβ7 heterodimer.[16–18] αEβ7 is exclusively expressed in immune cells and binds to the epithelial protein E-cadherin, mediating intraepithelial lymphocyte localization.[19]

CD103+ T_{RM} cells play an essential role in limiting tumor growth[20 21] as well as in immune surveillance of solid tumors.[22 23]

Consistent with these observations, tumor infiltration with CD103+ T_{RM} cells has been associated with better clinical outcomes in patients with lung, bladder, endometrial, gastric, and colorectal cancers receiving standard of care therapies.[10 22 24–28] Furthermore, CD103+ CD8+ T cells have been shown to preferentially localize in tumor epithelium compared with the surrounding stroma, with better patient outcomes observed with elevated T_{RM} cell frequency within tumor nests.[28–30] Expression of CD103 by T_{RM} cells is primarily induced by exposure to tissue-derived cytokines such as tumor growth factor β and interleukin-15.[31–34] However, it has been reported that T-cell receptor (TCR) engagement is also necessary to induce CD103 upregulation.[35 36] Thus, CD103+ tumor-infiltrating T cells may be the progeny of lymph node-activated and recirculating T effector (T_{EFF}) or T stem-cell memory (T_{SCM}) cells that have recently migrated into tumor tissues and differentiated as a result of exposure to these cytokines and tumor antigens.[37]

Elevated expression of immune checkpoint regulators such as PD-1 and TIM3 as well as enhanced proliferation (Ki-67) and activation (CD38) markers indicate that T_{RM} cells have the potential to actively limit tumor growth and play a key role in the response to cancer immunotherapy.[38] In addition, CD103+ CD8+ cells that coexpress CD39 (*ENTPD1*) have been found to be uniquely tumor reactive, while their CD39- counterparts are considered 'bystander' cells, often bearing TCRs specific for microbial antigens.[35 39] However, this observation remains controversial as other studies have found shared TCR clonotypes across different CD8+ T-cell subsets, implying ongoing differentiation between phenotypes within the tumor.[40] Importantly, CD39 expression also defines CD8+ T-cell clonotypes in tumors that are expanded and presumptively activated following anti-PD-1 therapy.[39 41] It thus seems possible that CD103+ T_{RM} cells are poised to respond to PD-1/PD-L1 blockade.[42] One recent study has demonstrated an association between the presence of CD103+ CD8+ T cells in lung tumors and patient response to checkpoint blockade.[43] However, the hypothesis that immune CD103 expression in tumors is predictive of response to cancer immunotherapy has not been comprehensively evaluated in large randomized clinical trials.

Our previous studies have identified clonally expanded CD8+ T_{EFF} cells in blood with shared clonotypes across both tumor and adjacent non-neoplastic tissues, suggesting that antitumor immunity is characterized by a continuous production of reactive T cells at sites external to the tumor.[44] These peripherally expanded T_{EFF} cells shared clonotypes with tumor T_{RM} cells, indicating differentiation of peripheral T_{EFF} into T_{RM} following migration into the tumor. Here, we expand on these studies by focusing on intratumoral T_{RM} cells and probe the relationships between CD8+ T-cell tumor infiltration, phenotype, proliferation, and clonal expansion using multidimensional approaches. Our analysis of a cohort of 1868 patients treated with the anti-PD-L1 antibody atezolizumab reveals that CD103 expression does indeed closely correlate with response to immunotherapy and highlights CD8+ T_{RM} as a critical player in the antitumor response.

MATERIALS AND METHODS

Human subjects

Samples analyzed from clinical trials were collected as prescreening biopsies obtained from archived paraffin-embedded tissue. Patients were required to have tissue sent to the central laboratory prior to entry into the study. Samples were processed at the time of screening. Tissue samples from three clinical trials were used for these analyses: (1) OAK (NCT02008227), a phase III randomized study comparing atezolizumab (anti-PD-L1 antibody, 1200 mg every 3 weeks) with docetaxel in patients with non-small cell lung cancer (NSCLC) after failure with platinum-containing chemotherapy; (2) IMvigor210 (NCT02108652), a single-arm phase II study investigating atezolizumab (1200 mg every 3 weeks) in patients with metastatic urothelial carcinoma (mUC); and IMvigor211 (NCT02302807), a phase III two-arm, randomized, controlled study comparing atezolizumab (1200 mg every 3 weeks) with chemotherapy (docetaxel, paclitaxel, or vinflunine) in subjects with locally advanced or mUC who have progressed during or following a platinum-containing regimen. Fresh tumor samples and matched adjacent non-cancerous tissues were procured from a commercial vendor (Discovery Life Sciences) as part of adult patients undergoing surgical resection. Online supplemental table S1 provides details for each individual sample such as age, gender, ethnicity, tumor stage, tumor histology subtype (if known), tumor area category (if known), extent of lymph node spread (if known), and metastatic status (if known). Adjacent tissue was required to be more than 0.5 cm away from the tumor and defined as being free of disease morphology at the discretion of the pathologist.

Statistical analysis

Comparisons across patient subgroups for *ITGAE* or CD103 immunohistochemistry (IHC) across CD8+ infiltration status (desert, excluded, and inflamed) as well as *ITGAE* by PD-L1 levels on immune cells (IC score) were completed using a Kruskal-Wallis test with a Dunn post hoc test adjusted with Benjamini-Hochberg correction for multiple comparisons. For statistical analysis of markers measured by mass cytometry between CD103+ and CD103– CD8+ subpopulations, a two-way analysis of variance with Bonferroni correction for multiple comparisons was used. Correlation of PD-L1 by mass cytometry with various gates of CD8+ T cells was assessed by a Spearman rank test. Statistical significance of differences in overall survival (OS) between patient groups subdivided by gene (*ITGAE* and *CD8A*) or protein (CD103) expression was determined by Cox proportional hazard modeling. For all statistical analyses, a p-value of <0.05 was indicated by '*', p<0.01 by '**', p<0.001 by '***',

p<0.0001 by '****' and lack of a significant difference by 'n.s.' (not significant).

Data and code availability

All data from bulk RNA sequencing (RNAseq) of patients from the IMvigor210 clinical trial were available within the European Genome–Phenome Archive (EGA) under accession number EGAS00001002556 and have also been previously published.[45] The resulting data from mass cytometry analyses are deposited in Flowrepository.org. Single-cell RNA sequencing (scRNAseq) and single-cell T cell receptor sequencing (scTCRseq) data used in these studies have previously been published[44] and are available within EGA under studies EGAS00001003993 and EGAS00001003994 and datasets EGAD00001005464 and EGAD00001005465. The bladder tumor dataset obtained from Oh *et al*[46] is publicly available in the NCBI GEO database under accession GSE149652. Coordinates for generation of the uniform manifold approximation and projection (UMAP) were obtained from the authors. There are restrictions to the availability of bulk RNAseq datasets from patients enrolled in OAK and IMvigor211 clinical trials, but a normalized expression matrix for *ITGAE* and *CD8A*, the only genes included from these trials in these studies, is provided in online supplemental data file S2.

RESULTS

Cohort characteristics

Clinical and biomarker data were obtained from 1868 patients within three clinical trials in two cancer indications assessing the clinical benefits of PD-L1 blockade with atezolizumab: IMvigor210—a single-arm, phase II study of atezolizumab in patients with first-line (n=95) or second-line (2L+, n=259) locally advanced or mUC[47]; IMvigor211—a two-arm, phase III randomized study in patients with 2L+ locally advanced or mUC comparing atezolizumab to chemotherapy[48]; and OAK—a two-arm, phase III randomized study in patients with 2L+ NSCLC comparing atezolizumab to docetaxel.[49] IHC for PD-L1 and CD8 as well as a bulk RNAseq analysis was performed on formalin-fixed paraffin-embedded (FFPE) tumor tissue obtained prior to administration of atezolizumab.

In parallel, independently of the clinical trials, six NSCLC and three endometrial tumor samples were procured as fresh tissue and both tumor and non-cancerous tumor-adjacent tissue were analyzed by mass cytometry, scRNAseq, and scTCRseq upon dissociation. Patient clinical and demographic information for these samples is detailed in online supplemental table S1.

Tumors with high CD8+ T-cell infiltration are enriched in CD103 (*ITGAE*) expression

Solid tumors have been categorized into inflamed, excluded, and desert phenotypes based on CD8+ T-cell infiltration patterns.[45 50] In inflamed tumors, CD8+ T cells penetrate tumor nests, while they are largely confined to the tumor stroma in excluded tumors. Tumors devoid of or with extremely low levels of CD8+ T cells are termed immune deserts. Transcriptional comparison of inflamed versus excluded tumors in IMvigor210 revealed 759 genes significantly overexpressed (adjusted p<0.05) in inflamed relative to excluded tumors, with *ITGAE* appearing as one of the most highly significant genes ($p=3.35\times10^{-18}$) (figure 1A and online supplemental data file S1). Other notable CD8+ T cell-associated genes such as *CD8A*, *IFNG*, and *LAG3* were also upregulated in inflamed tumors. Expression of the hallmark interferon (IFN)-inducible gene *GBP1* was also strongly associated with CD8 phenotype, indicative of ongoing IFN signaling in highly infiltrated tumors. Consistent with these findings and as expected, transcripts associated with T-cell cytokine production and activation pathways were significantly enriched in inflamed tumors, including type I and type II IFN as well as TCR and costimulation pathways (figure 1B).

Identification of the top 25 transcripts correlated with *ITGAE* expression in IMvigor210 yielded key genes associated with the T_{RM} phenotype as well as IFN-γ signaling (figure 1C). *CD8A* and *ZNF683*, which encodes HOBIT, a master regulator of T_{RM} differentiation,[18 51] were highly correlated with *ITGAE*, suggesting that CD8+ T_{RM} cells are likely the primary source of *ITGAE* in bulk tumor transcriptomes. *ITGAE* was highly correlated with *FASLG*, which is associated with TCR activation and can also be transcriptionally induced by type I IFN signaling.[52] Furthermore, *ITGAE* was also strongly correlated with the immune checkpoints *LAG3* and *PDCD1* (PD-1), as well as *IFNG*, the IFN-inducible gene *GBP5*, and IFN-γ-induced chemokines (*CXCL9*, *CXCL10*, and *CCL5*). Regulators of cytotoxic degranulation (*NKG7*) and genes encoding cytotoxic proteins (*PRF1*, *GZMA*, *GZMH*, and *GZMB*) were also associated with *ITGAE*.[53]

Increased *ITGAE* expression within inflamed tumors, relative to excluded and desert tumors, was observed in OAK (NSCLC, p=3.91e-42), IMvigor210 (mUC, p=1.78e-27), and IMvigor211 (mUC, p=8.58e-54) (figure 1D). *ITGAE* expression was also positively associated with PD-L1 levels on immune cells (IC score), a previously established biomarker of response to immunotherapy,[49] in all three trials (figure 1E). These observations were confirmed at the protein level by IHC for CD103 in FFPE tumor biopsies taken from a subset of patients from IMvigor210. Figure 1F shows representative images of hematoxylin-and-eosin (H&E) stained slides, and IHC for CD8 and CD103 performed on adjacent sections from tumor biopsies that correspond to each infiltration phenotype. Automated image analysis was used to quantify the prevalence of CD103+ cells within manually annotated tumor regions of interest. Supporting transcriptional observations, we found that CD103 staining was enriched in inflamed tumors relative to immune desert and excluded tumors (figure 1G). In summary, tumors infiltrated with CD8+ T cells expressed elevated levels of *ITGAE*/CD103 and were enriched in genes associated with TCR activation.

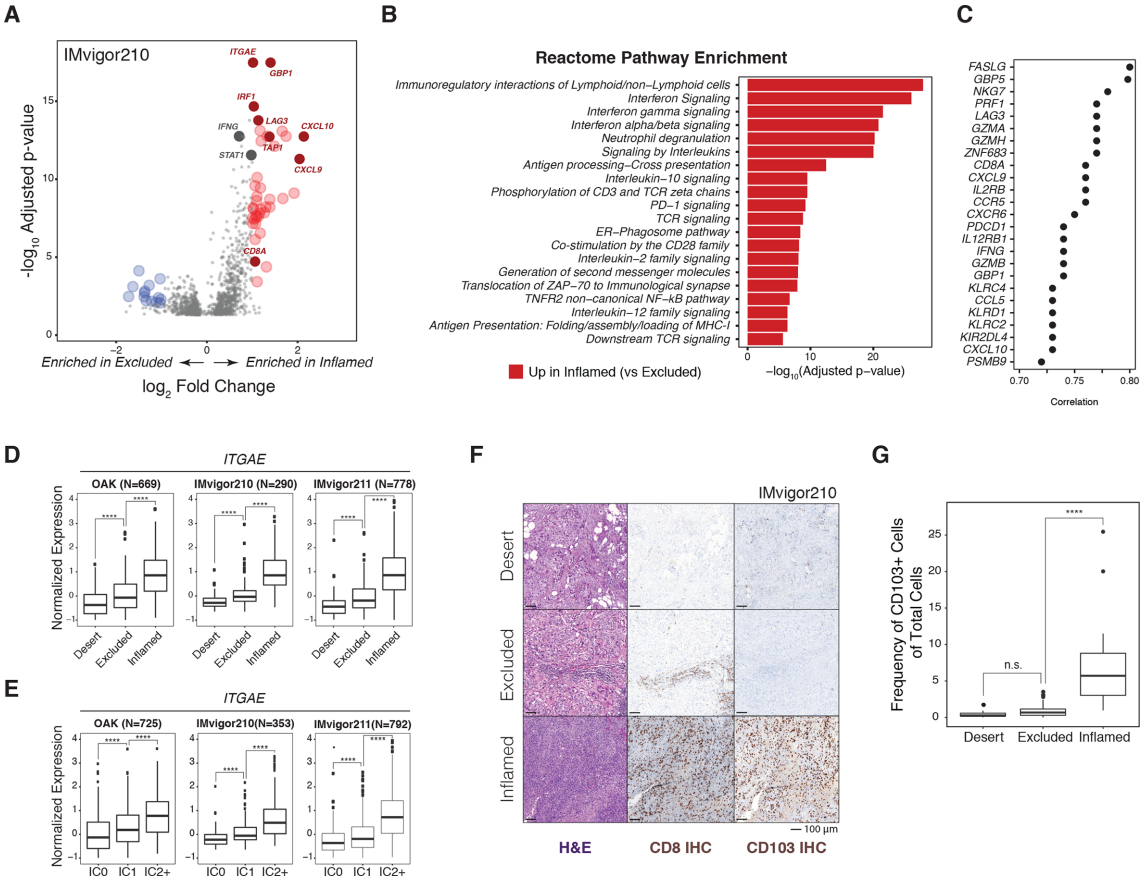

Figure 1 *ITGAE*/CD103 is upregulated in tumors exhibiting high CD8+ T-cell infiltration. (A) Volcano plot depicting differentially expressed genes between patients with inflamed versus excluded CD8+ T-cell infiltration phenotypes in tumors from the IMvigor210 clinical trial (mUC) (n=354). Colored dots indicate genes significantly (adjusted p value<0.05) upregulated (red, right) or downregulated (blue, left) greater than two-fold ($log_2FC \geq 1$) in inflamed relative to excluded tumors. Select genes representative of cytotoxic T cells and IFN signaling are annotated. (B) Top 20 reactome pathways enriched in inflamed tumors relative to excluded tumors ranked by significance ($-log_{10}$ (p-value) on x-axis). (C) Top 25 genes that correlate with *ITGAE* expression in a bulk RNAseq analysis of tumor samples from the IMvigor210 clinical trial. (D) Comparison of baseline *ITGAE* gene expression across patients categorized into desert, excluded, or inflamed subgroups based on CD8+ T-cell tumor infiltration patterns in three clinical trials: OAK (NSCLC, n=669), IMvigor210 (mUC, n=290), and IMvigor211 (mUC, n=778). Statistical analysis was conducted within each trial using the Kruskal-Wallis test with Dunn's post hoc test adjusted with Benjamini-Hochberg correction for multiple comparisons. (E) Box plots depicting *ITGAE* gene expression in bulk RNAseq profiles of tumors from OAK (n=725), IMvigor210 (n=353), and IMvigor211 (n=792) clinical trials categorized by low (IC0), mid (IC1), or high (IC2/3) PD-L1 expression on immune cells (IC) as measured by IHC. (F) Representative tissue imaging of FFPE tumors obtained from a subset of IMvigor210 patients (n=91) stained with H&E for tissue architecture (left), as well as for CD8 (middle, brown) and CD103 (right, brown) by IHC. (G) Comparison of CD103 IHC between desert (n=26), excluded (n=45), and inflamed (n=20) tumor infiltration phenotypes. Statistical analysis was completed using a Kruskal-Wallis test with Dunn's post hoc test adjusted with Benjamini-Hochberg correction for multiple comparisons. ****P<0.0001. FFPE, formalin-fixed paraffin-embedded; H&E, hematoxylin-and-eosin; IFN, interferon; IHC, immunohistochemistry; mUC, metastatic urothelial carcinoma; n.s., not significant; NSCLC, non-small cell lung cancer; PD-L1, programmed cell death ligand 1; RNAseq, RNA sequencing.

Intratumoral CD103+ CD8+ T cells express multiple immune checkpoints and Ki-67

To assess the prevalence, distribution, and phenotypes of CD103+ immune cells, a 38-parameter mass cytometry panel (online supplemental table S2) was applied to freshly dissociated tumors as well as non-cancerous tumor-adjacent tissue from six NSCLC and three patients with endometrial cancer. CD45+ cells from NSCLC tumors were merged to create a single UMAP of the immune microenvironment (figure 2A, left). T cells, B cells, NK cells, dendritic cells, macrophages, and neutrophils were identified with manual gates and projected onto the UMAP as previously described.[54] CD103 expression was primarily restricted to the CD8+ T-cell lineage but was also detectable in rare CD4+ T-cell and NK-cell subsets (figure 2A, right). Similar results were obtained for endometrial tumors (online supplemental figure S1A).

Manual gating analysis was performed on all tumors to quantify (1) the total immune cell composition for each tumor (online supplemental figure S1B, left), (2) the percentage of total CD103 expression attributable to each cellular lineage (figure 2B) and (3) the percent of cells expressing CD103 within each immune subpopulation (online supplemental figure S1B, right). As previously described in NSCLC[42] and bladder cancer,[24] while a small

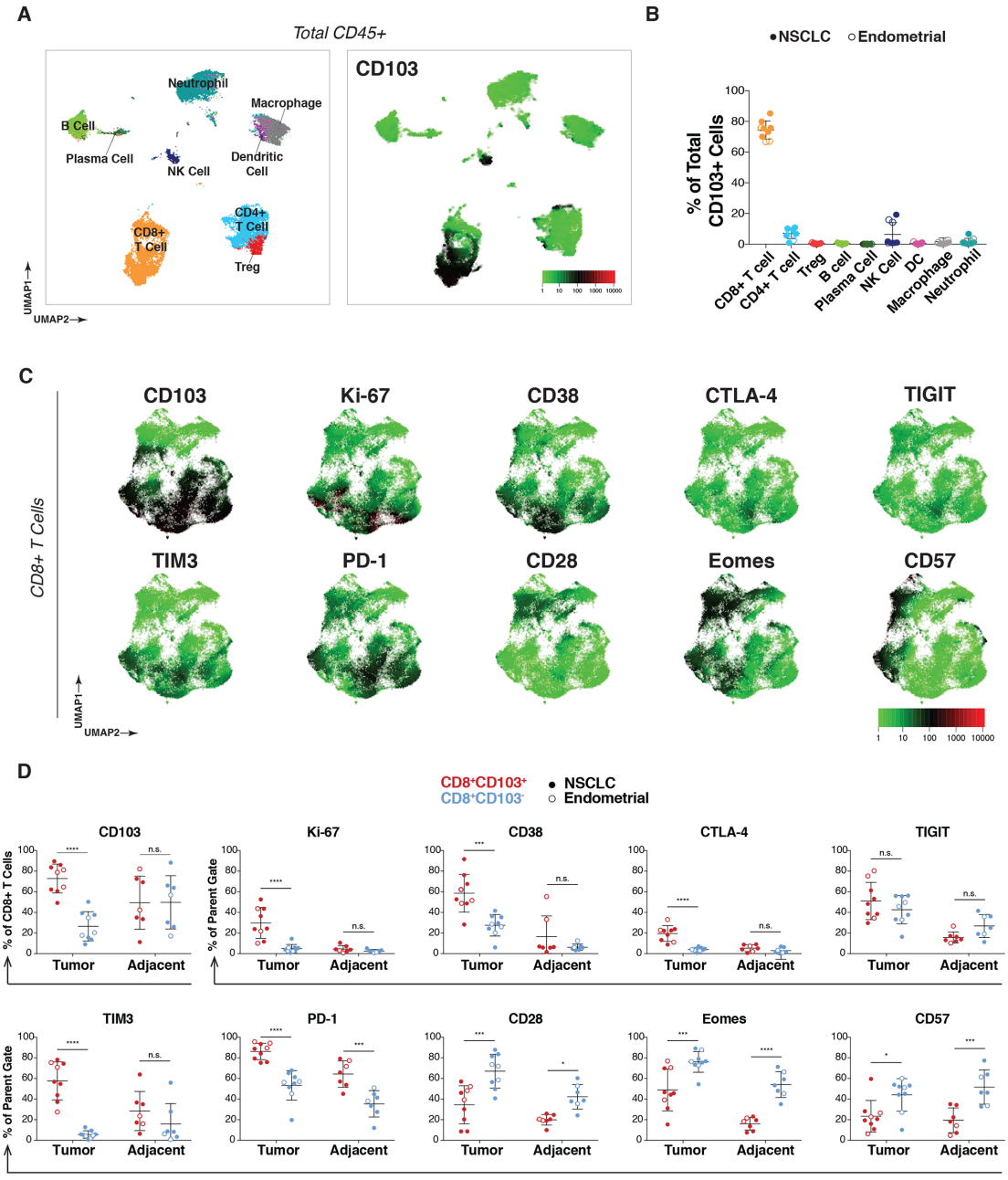

Figure 2 CD103+ cells in tumors are predominantly CD8+ T_{RM} cells and are characterized by Ki-67 and immune checkpoint expression. (A) NSCLC patient tumors (n=6) analyzed by mass cytometry, with resulting data for total CD45+ cells (8000 downsampled cells per sample) aggregated and visualized by UMAP (left). Immune subset identities were determined by manual gating and projected onto the UMAP. Expression of CD103 across total CD45+ cells from NSCLC tumors overlaid onto the UMAP (right). (B) Frequency of the indicated immune subpopulations of total CD103+ cells for all nine tumors (n=6 NSCLC (solid dots), n=3 endometrial cancer (open dots)). (C) Expression pattern for markers of activation and dysfunction for NSCLC tumors in aggregate projected onto the UMAP of CD8+ T cells. (D) Comparison of expression frequency of indicated markers within CD8+ T cells between CD103+ (red) or CD103– (blue) subsets in either tumor (left) or adjacent tissue (right) across all tumor samples (n=9, solid dots for NSCLC, open dots for endometrial). Statistical analysis was conducted using two-way analysis of variance with Bonferroni correction for multiple comparisons. *P<0.05, **P<0.01, ***P<0.001, ****P<0.0001. n.s., not significant; NSCLC, non-small cell lung cancer; PD-1, programmed cell death 1; T_{RM}, tissue-resident memory T; UMAP, uniform manifold approximation and projection.

subset of NK cells and CD4+ T cells express CD103, CD8+ T cells accounted for the majority of CD103+ immune cells in the tumor microenvironment (mean of 74%, range of 67%–85%).

Given the predominant expression of CD103 in CD8+ T cells and recent evidence that T_{RM} cells play a role in tumor immunity,[55] CD8 subsets were further investigated. CD8+ T cells from all samples were manually gated and merged to create a UMAP, revealing two major CD8+ T-cell populations

segregated by CD103 that were observed across all tumors analyzed (UMAPs by individual in online supplemental figure S1C, NSCLC tumors in figure 2C, and endometrial tumors in online supplemental figure S1D). Elevated expression of proliferation (Ki-67), activation (CD38), and immune checkpoint (CTLA-4, TIGIT, TIM3, and PD-1) markers was observed in CD103+ cells. In contrast, CD103− cells expressed higher levels of CD28, Eomesodermin (EOMES), and CD57. CD28 has been proposed as a marker of stem-like T cells based on TCF-1 and CD45RO expression in the context of renal cell carcinoma.[40]

We further quantified phenotypic differences between CD103+ and CD103− immune cells in tumors as well as non-cancerous tumor-adjacent tissue using manual gating analysis (figure 2D). CD103+ CD8+ T cells in the tumor were significantly enriched for Ki-67, CD38, CTLA-4, TIM3, and PD-1 expressing cells compared with CD103− CD8+ T cells. Few CD8+ T cells were found to express Ki-67, CD38, and CTLA-4 in adjacent tissue regardless of their CD103 phenotype, implying these markers may be associated with tumor-specific activation rather than exclusively being a result of their T_{RM} lineage. On the other hand, PD-1 was also elevated in CD103+ cells from adjacent tissues, suggesting some markers represent a tissue-specific rather than tumor-specific phenotype. In contrast, expression of CD28, EOMES, and CD57 were enriched in CD103− relative to CD103+ cells in both tumor and tumor-adjacent tissues. CD28 and EOMES are hallmarks of an effector memory CD8+ phenotype, with EOMES suppressing T_{RM} differentiation.[18 34] The enrichment for EOMES and CD57 in CD103− cells that expressed lower levels of inhibitory receptors was still somewhat unexpected as these markers also typically signify exhausted[3] and senescent[56] states, respectively. While both exhaustion and senescence are characterized by reduced effector function, the molecular pathways involved in these programs have been shown to differ.[57]

The percentage of total CD8+ T cells was not significantly correlated with PD-L1 expression on immune cells (CD45+) (online supplemental figure S1E). However, the frequency of CD103+ CD8+ T cells, and especially Ki-67+ CD103+ CD8+ cells, was significantly correlated with PD-L1 positivity on tumor-associated immune cells (p=0.0214 and p=0.0013, respectively), suggesting that this subpopulation could be responsible for inducing PD-L1 expression in the tumor microenvironment, for example, via the release of effector cytokines (eg, IFN-γ) that drive its expression.[58 59]

The association of CD103 expression with these phenotypic markers was also analyzed for CD4+ T cells as well as NK cells in tumor and tumor-adjacent tissue (online supplemental figure S2A,B). A smaller fraction of CD4+ T cells expressed CD103 (mean of 8.55% in tumor, 13.3% in adjacent) relative to the levels found in CD8+ T cells, consistent with previous observations.[60] In CD4+ T cells overall, Ki-67, CD38, CTLA-4, and TIGIT expressions were elevated in tumor relative to adjacent tissue, but these differences were not stratified by CD103 expression. Only EOMES and CD57 were elevated specifically in tumor CD103+ CD4+ T cells, the inverse of what was seen in tumor CD8+ T cells. NK cells were detected at low frequencies in tumor tissue and showed high variability in CD103 positivity (online supplemental figure S2B). CD57 was the only marker that matched what was observed for CD8+ T cells in the tumor for NK cells, where it was enriched in CD103− relative to CD103+ subpopulations; however, this was the case in adjacent tissue as well. In NK cells from adjacent tissue, significant differences based on CD103 expression were found for CD38, TIM3, and PD-1. Overall, CD8+ T cells were the most abundant CD103+ cell population we observed, and the presumably tumor-specific activated phenotype of CD103+ CD8+ T cells most likely reflects *in vivo* TCR triggering by tumor antigens.

CD8+ T_{RM} cells coexpress genes associated with dysfunction and cytotoxicity

In order to further characterize tumor CD8+ T-cell diversity and clonality, scRNAseq and scTCRseq were applied to a subset of the same samples analyzed by mass cytometry (NSCLC n=3, endometrial n=3). A UMAP was generated for tumor CD8+ T cells and annotated using cluster designations we previously defined (figure 3A).[44] Eight clusters were identified, capturing effector T cells (T_{EFF}, 8.1), effector memory T cells ($T_{EM,}$ 8.2), T_{RM} cells (8.3a-c), cells experiencing chromatin remodeling (8.4), mitotic cells (8.5), and KLRB1-expressing cells (8.6). Cluster annotations were cross-referenced with previous publications that revealed similar subpopulations with well-correlated gene signatures.[44] T_{RM} cells were the predominant CD8+ cell type present in the tumor, with 52.6% of cells falling in the 8.3a-c clusters combined (figure 3B, left panel, individual frequencies depicted in the right panel). Hierarchical clustering was used to visualize differential gene expression between clusters (figure 3C). 8.1-T_{EFF} cells were largely defined by the expression of the cytotoxic proteins *GZMB*, *GZMH*, and *PRF1*, as well as low levels of immune checkpoint regulators. Distinctively high levels of *GZMK* were observed in 8.2-T_{EM} along with coexpression of *TNF*, *CD27*, *CD28*, and *EOMES*, indicative of an effector memory phenotype.[61] The cluster identified as 8.4-Chrom was previously characterized as being involved in chromatin remodeling and ongoing histone modification, as evidenced by expression of chromatin remodeling enzyme *CHD1* and long non-coding RNA *MALAT1*, which directly binds components of the chromatin remodeling complex.[62] The 8.6-KLRB1 cluster exhibited uniquely high levels of *KLRB1*, along with *TCF7*, *CCR7*, and *IL7R*, indicating the possibility that this cluster represents T_{SCM} cells, a population thought to be essential for response to checkpoint inhibition when harboring TCRs specific to tumor antigens.[63] Importantly, 21% of cells in cluster 8.6 expressed the TRAV1-2 conserved TCR domain, which is a marker of the mucosal associated invariant T-cell lineage, thus suggesting even deeper phenotypic diversity within this cluster.[64]

Three distinct T_{RM} clusters (8.3a-c) were found to be stratified by a stepwise increase in *ITGAE* along with immune checkpoint regulators, *IFNG*, *CXCL13*, and multiple cytotoxic proteins (figure 3C). *ZNF683*, the gene encoding HOBIT, was expressed in all three

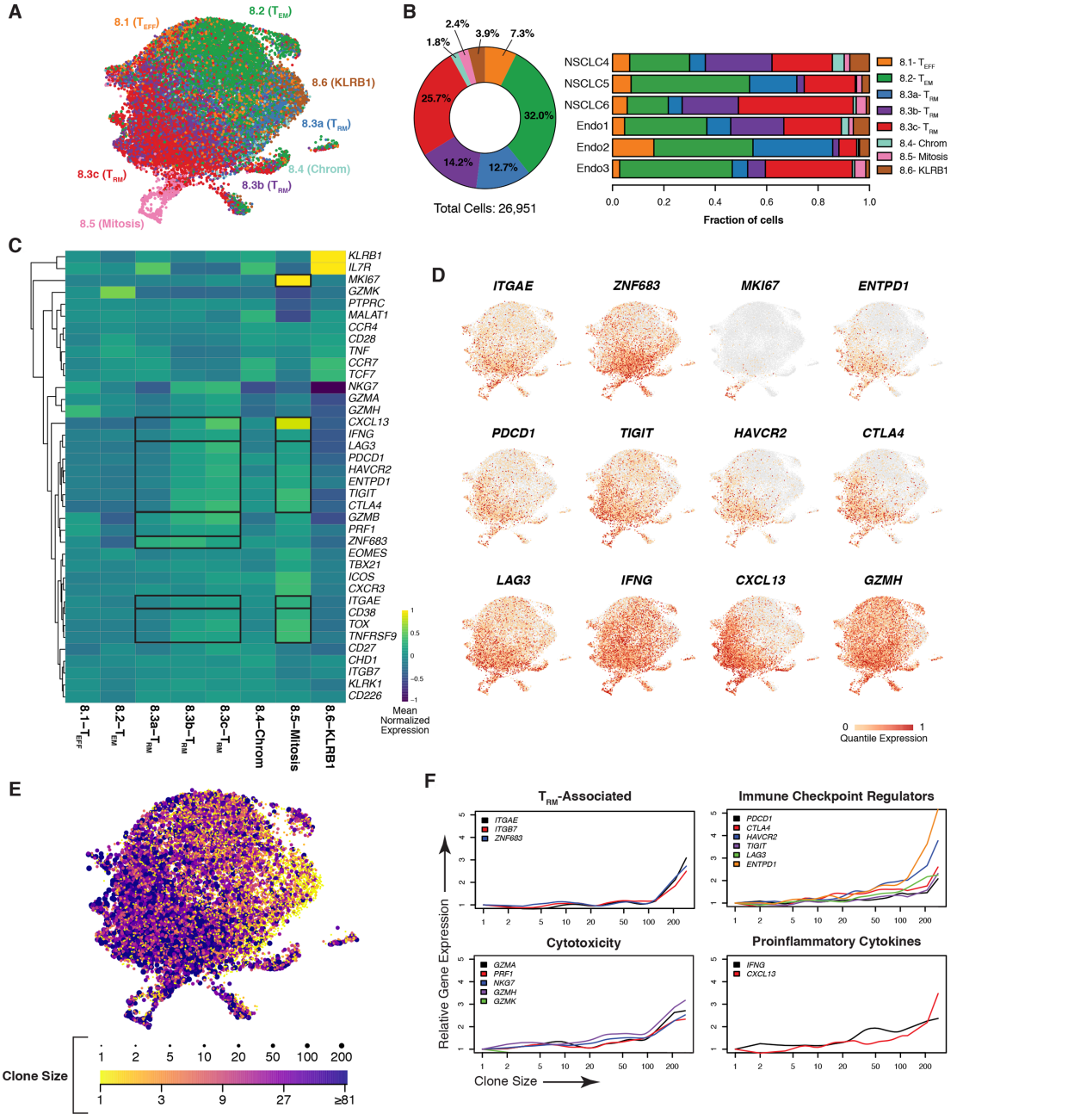

Figure 3 Tumor CD8 +T_{RM} cells are clonally expanded and express genes associated with cytotoxicity and dysfunction. (A) UMAP of CD8+ T cells from NSCLC (n=3) and endometrial (n=3) tumor samples with clusters colored by subset identity as analyzed by scRNAseq. (B) Frequency of each CD8+ T-cell cluster among all tumors assessed with samples in aggregate (left) or by individual (right). (C) Heatmap depicting relative expression of T cell-associated genes, with a dendogram indicating results of hierarchical unsupervised clustering (left), across CD8+ clusters. Genes are globally scaled with an expression range from −1 (dark blue) to 1 (yellow). (D) UMAP overlay of genes associated with the T_{RM} phenotype, proliferation, dysfunction, as well as genes correlated with *ITGAE* in the bulk RNAseq and heatmap analyses. Individual cells are colored on a scale of gray (0) to red (1) according to the quantile of their expression. (E) Extent of clonal expansion, as determined by scTCRseq, for each cell overlaid onto the UMAP (A). The breadth of TCR clonality is represented by dot size and by color, ranging from a clone size of 1 (yellow) to greater than 81 (purple). (F) Expression of indicated genes (y-axes) as a function of the size of a given clonotype (with clone size rank ordered on the x-axis) for resident memory T-cell phenotype, checkpoint regulator, cytotoxicity, and proinflammatory cytokine genes. NSCLC, non-small cell lung cancer; RNAseq, RNA sequencing; scRNAseq, single-cell RNA sequencing; scTCRseq, single-cell TCR sequencing; TCR, T-cell receptor; T_{RM}, tissue-resident memory T; UMAP, uniform manifold approximation and projection.

clusters but appeared highest in 8.3a and 8.3b. T_{RM} cluster 8.3a could represent a transitional state between progenitor phenotypes and T_{RM} differentiation as tissue residency and stem-like markers (eg, *IL7R*) overlapped in this population.[33] Cluster 8.3a may also be resting T_{RM} bystander cells. Relatedly, the transcription factor TOX

has emerged as a master regulator of exhaustion; thus, its expression is capable of delineating chronically activated tumor antigen-specific T cells from bystanders.[65 66] Importantly, TOX programming also inhibits clonal deletion, enabling cellular persistence.[66] *TOX* expression was absent in cluster 8.3a but increased progressively in clusters 8.3b and 8.3c. As anticipated by recent studies, *TOX* expression in 8.3b and 8.3c overlapped with phenotypic markers of T-cell dysfunction as well as the ATPase *ENTPD1* (CD39), another putative marker of tumor-specific CD8+ T cells.[35]

Our mass cytometry analysis demonstrated that a subset of CD103+ CD8+ T cells displayed Ki-67 expression (figure 2C,D), suggesting a proliferative state. While cluster 8.3a-c did not express *MKI67*, a separate cluster 8.5 expressed high levels of *MKI67* and also had the highest expression of *ITGAE* across all clusters, as well as robust expression of checkpoint molecules, *TOX*, and *ENTPD1* (figure 3C). Importantly, these mitotic T_{RM} cells also displayed elevated expression of *IFNG*, the TCR activation-specific marker *TNFRSF9* (4-1BB), and *CXCL13*, which collectively may signify response to tumor antigens *in vivo* prior to tumor excision.

In order to precisely assess the relationship between CD103 and CD39 expression, mass cytometry was applied to a pair of matched NSCLC tumor and adjacent tissue samples (online supplemental figure S3A). Like Ki-67, CD39 was selectively expressed on intratumoral CD103+ cells, with fivefold less CD39+ CD103+ cells detected in the adjacent tissue (online supplemental figure S3B). Furthermore, manual gating analysis showed that CD39+ CD8+ T cells were a subset of CD103+ cells (online supplemental figure S3C). Ki-67 and checkpoint regulators were enriched in CD103+ CD39+ cells relative to CD103+ CD39- cells (online supplemental figure S3D,E). CD103– CD39– T cells exhibited the lowest frequency of positivity for these markers and instead were elevated in positivity for CD28, EOMES, and CD57 (online supplemental figure S3D,E).

Transcript levels for specific genes of interest were displayed via UMAP in order to visualize their expression with single-cell resolution (figure 3D and online supplemental figure S4A). *ITGAE*, *ZNF683*, and *ENTPD1* were most localized in the T_{RM} and mitotic clusters. T_{RM} clusters were enriched in checkpoint regulators, *IFNG*, *CXCL13*, and cytotoxicity mediators (eg, *GZMH*, *GZMA*, and *GZMB*), whereas *MKI67* positivity was only observed in the mitotic subset of T_{RM} (8.5). Conversely, *GZMK* was expressed outside of T_{RM} clusters in T_{EM} cells (online supplemental figure S4A). Online supplemental figure 4 depicts UMAP visualizations for additional genes of interest that were presented in our heatmap and mass cytometry analyses.

Tumor T_{RM} cells exhibit clonal expansion

Single-cell TCR clonality analysis was then performed to associate cellular phenotypes with patterns of clonal expansion. Overlaying clone size onto the UMAP (represented by both data point size and color), we observed that cells with high degrees of clonal expansion were mostly localized in the 8.3c-T_{RM} cluster (figure 3E). Comparing gene expression to clone size in a quantitative manner, we found that T_{RM}-associated genes (*ITGAE*, *ITGB7*, and *ZNF683*) were most expressed in expanded clonotypes (figure 3F). Expression of checkpoints, cytotoxic molecules, and proinflammatory cytokines appeared highest in these clones, although they were also detected to a lesser extent on smaller clonotypes. In contrast, *GZMK* (figure 3F) along with genes associated with a naive or stem-like T-cell state (*IL7R*, *CCR7*, and *TCF7*) (online supplemental figure S4B) were primarily expressed in cells with the least number of clones.

TCR clonotype sharing between clusters (light gray columns) was broadly observed, although with variable frequency, suggesting phenotypic plasticity (online supplemental figure S4C). Clusters 8.3b and 8.3c shared TCRs, indicating potential intratumoral lineage differentiation. However, some clones (black columns) were more restricted to specific clusters. Importantly, mitotic cluster 8.5 shared clonotypes primarily with the T_{RM} clusters, further supporting the relationship between *in vivo* proliferation and the tissue-resident phenotype.

Taken together, this suggests that the previously identified TCR activation signatures in inflamed tumors (figure 1B) and CD8+ T_{RM}-specific Ki-67 expression (figure 2D) can result in T_{RM} cell proliferation *in vivo*. Furthermore, increased cytolytic protein expression in T_{RM} cells as a function of clonal expansion may reflect the ability of these cells to control tumor growth, as has been described in preclinical models.[20 21] These observations are aligned with previous scRNAseq analyses of the lung[67] and skin[68 69] tumor microenvironment with the additional insight provided here that the cell populations annotated as exhausted in these previous studies are most likely T_{RM} cells.

Reanalysis of a recently published scRNAseq dataset of T cells in bladder cancer[46] identified a CD8+ T-cell subpopulation expressing CD39 transcripts (annotated as $CD8_{ENTPD1}$) that closely resembled the phenotype we observed in 8.3c-T_{RM} cells (comparative cluster analysis in online supplemental figure S5A). In addition, this study also found a proliferative CD8+ population that correlated to the mitotic T_{RM} cells in cluster 8.5 (online supplemental figure S5A,B). However, relative frequencies of the various CD8+ clusters differed from our observations in NSCLC (online supplemental figure S5C).

ITGAE/CD103 expression predicts clinical response to immunotherapy

The association between *ITGAE* expression in pretreatment tumor biopsies and overall survival (OS) was assessed in the OAK, IMvigor210, and IMvigor211 cohorts. In OAK, increased OS was observed in $ITGAE^{high}$ tumors from patients treated with atezolizumab but not chemotherapy (figures 4A and online supplemental figure S6A), with *CD8A* behaving similarly. When looking at the prognostic capacity of *ITGAE* in mUC, we again observed that

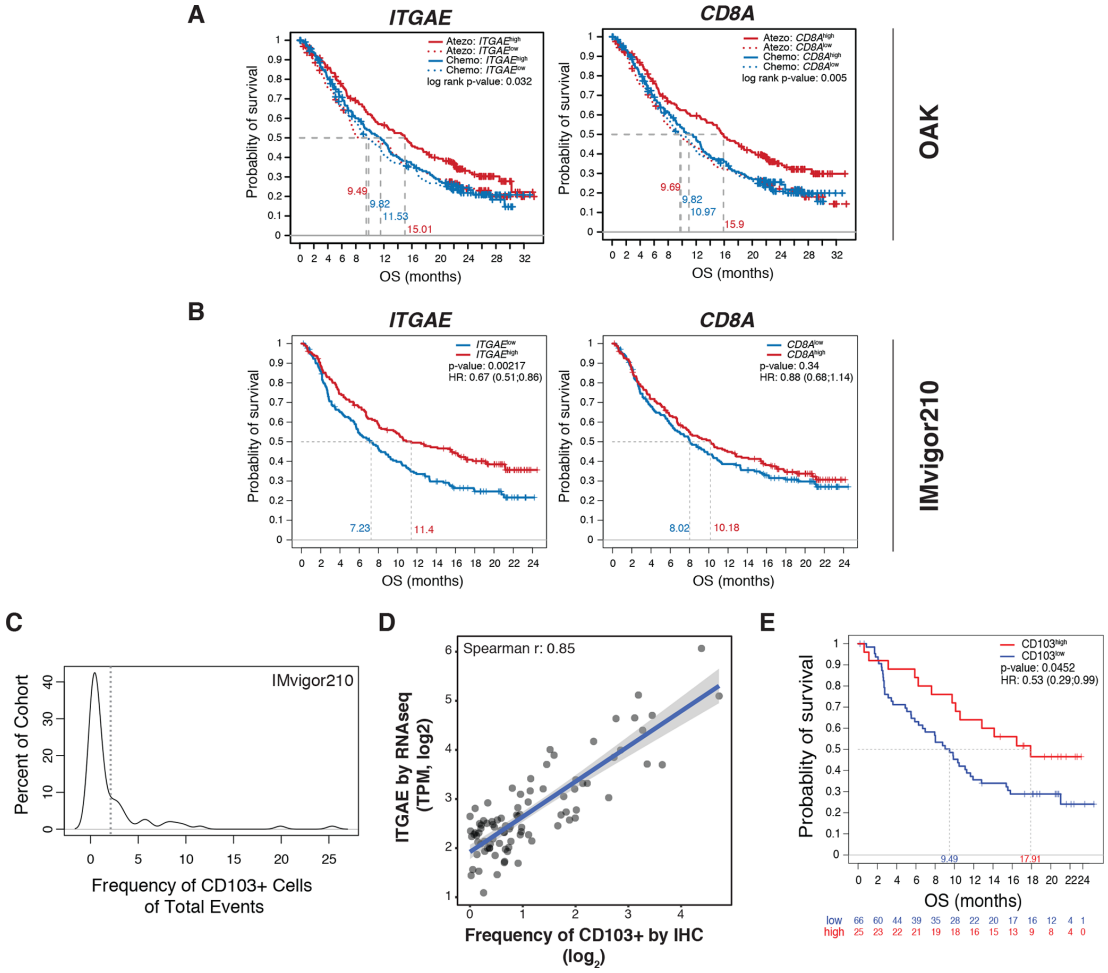

Figure 4 *ITGAE*/CD103 expression is predictive of response to PD-L1 blockade. (A) Kaplan-Meier curves depicting the OS probability of patients with locally advanced or metastatic NSCLC cancer treated with atezolizumab (red) or chemotherapy (blue) (OAK) categorized by high (solid line) or low (dotted line) transcriptional expression (median cut-off) of either *ITGAE* (left panel) or *CD8A* (right panel). P-values are displayed within each panel. (B) Kaplan-Meier curves demonstrating OS in patients with mUC from IMvigor210 categorized by high (red) or low (blue) transcriptional expression (median cut-off) of either *ITGAE* (left panel) or *CD8A* (right panel). HRs and p-values are shown for each gene. (C) Distribution of CD103+ cells in the tumor area across a subcohort (n=91) of IMvigor210 biopsies stained for CD103 by IHC. The dotted line indicates the 2% cut-off defining $CD103^{high}$ and $CD103^{low}$ patient groups. (D) Correlation of gene expression of *ITGAE*, as measured by bulk RNAseq analysis (TPM, y-axis), to quantification of CD103 protein by IHC (frequency of positive events out of total cells in tumor area, x-axis) for the subset of IMvigor210 patient samples analyzed. The Spearman R correlation value is displayed on the graph. (E) Kaplan-Meier curves comparing OS for patients defined as $CD103^{high}$ and $CD103^{low}$ in (C). Statistical significance was determined by Cox proportional hazard modeling. The HR and p-value are displayed within. HR, hazard ratio; IHC, immunohistochemistry; mUC, metastatic urothelial carcinoma; NSCLC, non-small cell lung cancer; OS, overall survival; PD-L1, programmed cell death ligand 1; RNAseq, RNA sequencing; TPM, transcripts per million.

patients with $ITGAE^{high}$ tumors treated with atezolizumab had significantly increased OS relative to their $ITGAE^{low}$ counterparts (IMvigor210) (figure 4B and online supplemental figure S6B). Remarkably, high *CD8A* expression was not associated with increased OS in this cohort. In the randomized trial IMvigor211, $ITGAE^{high}$ tumors demonstrated a modest improvement in OS compared with $ITGAE^{low}$ tumors in patients treated with atezolizumab but not chemotherapy (online supplemental figure S6C), with the highest quartile demonstrating a trend toward increased OS in the atezolizumab-treated arm (online supplemental figure S6D), a phenomenon not observed with *CD8A*.

CD103 IHC was then performed on a subset of tumors from IMvigor210 (n=91) to verify association with clinical outcome at the protein level. Based on the distribution of CD103+ cells in the tumor area across these patients, a ≥2% cut-off was selected for CD103 positivity (figure 4C). The frequency of CD103+ cells was correlated with *ITGAE* gene expression, as determined by bulk RNAseq (figure 4D). Patients were separated into $CD103^{low}$ and $CD103^{high}$ subgroups, based on the ≥2% cut-off identified. $CD103^{high}$ patients (median OS: 17.9 months) demonstrated improved OS (HR=0.53, p=0.045) relative to $CD103^{low}$ individuals (median OS: 9.5 months) (figure 4E). Thus, at both the transcriptional and protein

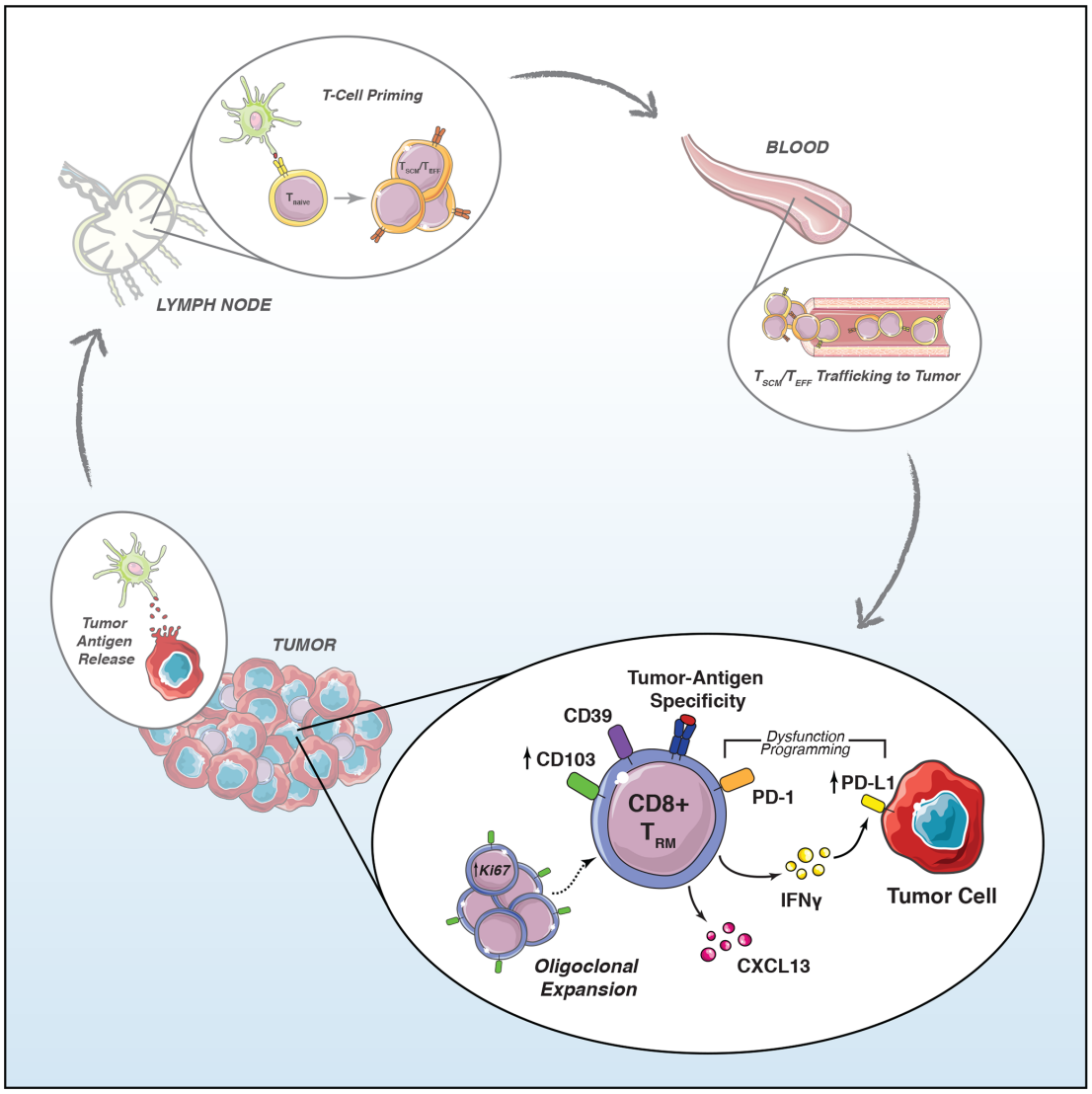

Figure 5 Activated tumor antigen-specific CD103+ T_{RM} cells generate biomarker signals of immunotherapy response. PD-1, programmed cell death 1; PD-L1, programmed cell death ligand 1; T_{EFF}, effector T; T_{RM}, tissue-resident memory T; T_{SCM}, stem cell memory T.

levels, CD103 expression in tumors was associated with better OS in patients treated with atezolizumab.

DISCUSSION

Tumor infiltration by CD8+ T cells is an essential step of the cancer immunity cycle.[70] Recent single-cell studies have identified multiple subsets of intratumoral CD8+ T cells, including T_{RM} cells which express high levels of checkpoint regulators, leading to their characterization as being either exhausted[9] or dysfunctional.[69] The functionality of tumor-infiltrating CD8+ T cells is controversial, and the relationships between exhausted and tissue-resident T cells remain poorly understood.[71] Here, we show that T-cell exhaustion is associated with a tissue resident phenotype. Based on these observations, we propose a model (figure 5) whereby in the development of anti-tumor immunity, tumor antigen presentation and lymph node activation of T_{SCM} cells lead to T_{EFF} cell egress from lymph nodes and circulation into tumor tissue via blood. In response to tumor antigens and cytokines present in the tumor environment, these cells differentiate into T_{RM} cells and secrete IFN-γ, causing the upregulation of IFN-γ-inducible genes such as PD-L1.[37] The interplay between tumor reactive T_{RM} activity and the paracrine induction of PD-L1 in tumor and antigen-presenting cells thus forms the basis of PD-L1-dependent adaptive immune resistance[59 72] and may act to prevent activation-induced T-cell death.[66] As such, PD-L1 biomarker status may indicate the existence of an ongoing CD103+ CD8+ T-cell immune response, consistent with our observed correlation between the frequency of Ki-67+ CD8+ T_{RM} and PD-L1+ immune cells (online supplemental figure S1E).

While T_{RM} tumor reactivity can be inferred based on overt phenotypic signs of chronic stimulation, the presumed dysfunctionality of these cells makes it unclear

whether T_{RM} activity is a proximal or distal biomarker relative to the unknown precise mode of action of PD-1/PD-L1 blockade. In a 'reinvigoration' or reversible exhaustion model, PD-1/PD-L1 checkpoint inhibition should function optimally in tumors infiltrated with exhausted cells. However, multiple studies suggest the presence of an epigenetically programmed terminally exhausted state enforced by TOX that is induced early upon chronic stimulation and unlikely to be reversible.[73 74] Alternatively, it has been shown in preclinical models that PD-1/PD-L1 checkpoint inhibition acts on self-renewing T_{SCM} cells,[75 76] but the precise differentiation state and physiological compartment that immune checkpoint inhibition targets for clinical efficacy remains obscure. Importantly, multiple functional studies suggest that simply the expression of immune checkpoint regulators such as PD-1, TIM3, and LAG3 is insufficient in identifying cells that are inert or terminally exhausted and that CD8+ T cells expressing these markers produce the same, if not more, inflammatory cytokines than cells lacking checkpoints.[77–81] Furthermore, tumor CD8+ T_{RM} cells uniquely expressed *CXCL13* (figure 3C,D), which has been shown in multiple studies to be a distinct functionality of 'exhausted' CD8+ T cells.[3 82] CXCL13 can contribute to tertiary lymphoid structure formation, which has been recently linked to immunotherapy response.[83] Precise identification of the subset and phenotypic state that is most poised to directly respond to immunotherapy will require further investigation, though our study and others point to a potential role for tumor CD8+ T_{RM} cells.

Recent studies have shown that following anti-PD-1 therapy, novel tumor antigen-specific (based on CD39 expression) TCR clones are expanded rather than clones that had been detected prior to treatment.[41] The phenomenon of clonal replacement following checkpoint therapy does not preclude a 'pre' or 'progenitor' exhaustion model in which T cells that are clonally expanded in the tumor prior to treatment are still a relevant direct target of PD-1/PD-L1 blockade. Pre-exhausted cells may be 'potentiated' and rescued from terminal exhaustion by immune checkpoint inhibition. Rather than being reinvigorated, implying further clonal expansion, pre-exhausted T_{RM} cells already proliferating and involved in tumoricidal activity could potentially break the cycle of adaptive immune resistance induced by PD-1 signaling without expanding dramatically in numbers post-treatment. Potentiated tumor lysis could provide new tumor antigens (epitope spread) for dendritic cell capture in draining lymph nodes, subsequently generating a systemic immune response resulting in tumor infiltration with novel TCR clones. It is possible that sustained T_{RM}-mediated antitumor activity causes clonal replacement to be a constant feature of the cancer immunity cycle that is accelerated, rather than induced *de novo*, by immune checkpoint inhibition.

Importantly, tumor signatures of immune reactivity or 'exhaustion' have not universally correlated with improved clinical outcomes.[4–8] Studies in melanoma found patients with high numbers of TCF-1+ T_{SCM} cells and low numbers of exhausted cells to have better outcomes than patients in whom this ratio is inverted.[9] However, the T_{SCM} phenotype, in contrast to tumor T_{RM} cells, does not overtly display hallmarks of cellular activation, and thus tumor reactivity cannot be assumed unless proven by other methods.[71] In highly immunogenic tumors, it is possible that a large fraction of CD8+ T cells, including T_{SCM} cells, are tumor antigen-specific and poised to respond to checkpoint inhibition, but it is as yet unclear whether tumor T_{SCM} content can serve as a biomarker in indications other than melanoma. In contrast, the T_{RM} phenotype, and CD103 specifically, has been associated with improved OS in several cancers.[10 84] Our data revealed potential indication-specific differences in the predictive utility of *ITGAE* relative to *CD8A* (figure 4). This could reflect phenotypic differences in predominant CD8+ T cells between tumor types. In NSCLC, where both genes showed similar associations with OS (figure 4A), we observed a very high overlap of CD103 and CD8 (online supplemental figure S1B). In mUC, CD8+ CD103+ T_{RM} cells were present at reduced frequencies relative to NSCLC (online supplemental figure S5C); thus, the elevated presence of CD8+ CD103− bystander cells may explain the superiority of *ITGAE* over *CD8A* as a biomarker of clinical response in this indication. As such, response to immunotherapy is not only connected to the extent of CD8+ T-cell infiltration in inflamed versus excluded tumors but also the quality and phenotype of the cells present. Our initial observation that classification as an inflamed tumor was closely tied to CD103 expression highlights these cells as key players in antitumor responses. The routine inclusion of CD103 as an immunotherapy biomarker will enable the extension of these observations to other indications that remain largely unexplored in this context such as pancreatic cancer, renal cell carcinoma, and lymphomas. Furthermore, we believe the quantification of proliferative (or Ki-67+) CD103+ T_{RM} cells will have additional value in that these cells may be most proximal to the method of action of PD-L1 blockade and thus highly predictive of immunotherapy response.

Our studies have focused on T_{RM} cells specifically within the primary tumor tissue. With the development and control of metastases being of significance to patient prognosis, a key question is whether CD103+ tumor antigen-specific T_{RM} cells are able to leave the tumor and circulate to these secondary metastases or whether their tissue specificity is permanent. Recent preclinical evidence suggests that rather than being confined to tissue as a terminal state, T_{RM} cells maintain plasticity and can rejoin the circulating pool of T cells as conventional memory cells.[85] Identifying the phenotypes, clonality, and interplay of CD8+ T cells in these distant metastases will be of great importance in determining the long-term impact of T_{RM} cells on cancer survival outcomes.

Overall, we have identified CD103 as a marker of CD8+ T-cell tumor infiltration, and demonstrated that these

cells exhibit an activated and proliferative phenotype characterized by clonal expansion. CD103 expression, both at the transcriptional and protein levels, associates with better response to checkpoint blockade. Future studies will be necessary to determine whether T_{RM} activity is a proximal or distal biomarker of immune checkpoint inhibition and how exactly these cells contribute to anti-tumor responses post-therapy. Further reading material are listed in the supplemental material provided.[86–97]

Author affiliations
[1]Department of Oncology Biomarker Development, Genentech Inc, South San Francisco, California, USA
[2]Department of Cancer Immunology, Genentech Inc, South San Francisco, California, USA
[3]Department of Research Pathology, Genentech Inc, South San Francisco, California, USA
[4]Department of Bioinformatics and Computational Biology, Genentech Inc, South San Francisco, California, USA
[5]Adaptive Biotechnologies Corp South San Francisco, South San Francisco, California, USA
[6]Department of OMNI Biomarker Development, Genentech Inc, South San Francisco, California, USA
[7]Department of Microchemistry, Proteomics, Lipidomics, and Next Generation Sequencing, Genentech Inc, South San Francisco, California, USA
[8]Analytical Biosciences Limited, South San Francisco, California, USA
[9]Ventana Medical Systems Inc, Tucson, Arizona, USA
[10]Bolt Biotherapeutics, Redwood City, California, USA
[11]Department of Biostatistics Oncology, Genentech Inc, South San Francisco, California, USA
[12]Foundation Medicine, Cambridge, USA
[13]Barts Cancer Center, Queen Mary University, London, UK

Acknowledgements We thank Valerie Quarmby, Hanjo Lim, Bartek Bossak, Jose Diaz, Paul Vu, Justin Low, Mehraban Khosraviani, and Mike Phan for mass cytometry reagent support. We acknowledge SMART-servier for provision of graphic components used in the generation of the model figure. We thank Mary Keir for discussions on Integrin αE. We also thank Suvasha Gupta, Susan Flynn, and the Biosample Repository and Human Tissue Labs for tissue sample logistical support. We thank David Oh for providing dimensionality reduction coordinates for the bladder data.

Contributors Conceptualization: RB, ASC, SM, JG and WOG; validation, RB and WOG; formal analysis: RB, ASC, NSP, TDW, AA-Y, JCH, WZ, EAE-G, HK and WOG; investigation: ASC, AS, PdA, SM, AA-Y, CT, Y-JC and MDR; resources: TP, ZM, EEK and PC; writing of the original draft: WOG, ASC and RB; writing (review and editing): all authors; visualization: RB, ASC, AS, TDW, STE and AA-Y; supervision: PSH, IM, WRM, JMcB and TP; project administration: RN, MK, MMcM, WZ, SM. AS, TDW and NSP were co-second authors.

Funding The authors have not declared a specific grant for this research from any funding agency in the public, commercial or not-for-profit sectors.

Competing interests All authors except Thomas Powles are current or former employees of Roche.

Patient consent for publication Not required.

Ethics approval The authors complied with all ethical standards of the Roche Ethics Committee. Informed consent was obtained from all sampled individuals.

Provenance and peer review Not commissioned; externally peer reviewed.

Data availability statement Data are available in a public, open access repository. All data relevant to the study are included in the article or uploaded as supplementary information. All data from bulk RNA sequencing (RNAseq) of patients from the IMvigor210 clinical trial are available within the European Genome-Phenome Archive under accession number EGAS00001002556 and have also been previously published. The resulting data from mass cytometry analyses are deposited in Flowrepository.org. Single-cell RNA and TCR sequencing data used in these studies have previously been published and are available within EGA under studies EGAS00001003993 and EGAS00001003994 and datasets EGAD00001005464 and EGAD00001005465. The bladder tumor dataset obtained from Oh et al., 202061 is publicly available in the NCBI GEO database under accession GSE149652. Coordinates for generation of the UMAP were obtained from the authors. There are restrictions to the availability of bulk RNAseq datasets from patients enrolled in OAK and IMvigor211 clinical trials, but a normalized expression matrix for ITGAE and CD8A, the only genes included from these trials in these studies, is provided as a supplementary file.

ORCID iD
William E O'Gorman http://orcid.org/0000-0003-0753-3355

REFERENCES

1 Pauken KE, Wherry EJ. Overcoming T cell exhaustion in infection and cancer. *Trends Immunol* 2015;36:265–76.
2 Gong J, Chehrazi-Raffle A, Reddi S, *et al*. Development of PD-1 and PD-L1 inhibitors as a form of cancer immunotherapy: a comprehensive review of registration trials and future considerations. *J Immunother Cancer* 2018;6:8.
3 van der Leun AM, Thommen DS, Schumacher TN. $CD8^+$ T cell states in human cancer: insights from single-cell analysis. *Nat Rev Cancer* 2020;20:218–32.
4 Verma V, Shrimali RK, Ahmad S, *et al*. PD-1 blockade in subprimed CD8 cells induces dysfunctional $PD\text{-}1^+CD38^{hi}$ cells and anti-PD-1 resistance. *Nat Immunol* 2019;20:1231–43.
5 Mazzaschi G, Madeddu D, Falco A, *et al*. Low PD-1 expression in cytotoxic $CD8^+$ tumor-infiltrating lymphocytes confers an immune-privileged tissue microenvironment in NSCLC with a prognostic and predictive value. *Clin Cancer Res* 2018;24:407–19.
6 Kim H-D, Song G-W, Park S, *et al*. Association between expression level of PD1 by tumor-infiltrating $CD8^+$ T cells and features of hepatocellular carcinoma. *Gastroenterology* 2018;155:1936–50.
7 Ma J, Zheng B, Goswami S, *et al*. $PD1^{Hi}$ $CD8^+$ T cells correlate with exhausted signature and poor clinical outcome in hepatocellular carcinoma. *J Immunother Cancer* 2019;7:331.
8 Datar I, Sanmamed MF, Wang J, *et al*. Expression analysis and significance of PD-1, LAG-3, and Tim-3 in human non-small cell lung cancer using spatially resolved and multiparametric single-cell analysis. *Clin Cancer Res* 2019;25:4663–73.
9 Sade-Feldman M, Yizhak K, Bjorgaard SL, *et al*. Defining T cell states associated with response to checkpoint immunotherapy in melanoma. *Cell* 2018;175:998–1013.
10 Amsen D, van Gisbergen KPJM, Hombrink P, *et al*. Tissue-resident memory T cells at the center of immunity to solid tumors. *Nat Immunol* 2018;19:538–46.
11 Masopust D, Soerens AG. Tissue-resident T cells and other resident leukocytes. *Annu Rev Immunol* 2019;37:521–46.
12 Farber DL, Yudanin NA, Restifo NP. Human memory T cells: generation, compartmentalization and homeostasis. *Nat Rev Immunol* 2014;14:24–35.
13 Fransen NL, Hsiao C-C, van der Poel M, *et al*. Tissue-resident memory T cells invade the brain parenchyma in multiple sclerosis white matter lesions. *Brain* 2020;143:1714–30.
14 Sasson SC, Gordon CL, Christo SN, *et al*. Local heroes or villains: tissue-resident memory T cells in human health and disease. *Cell Mol Immunol* 2020;17:113–22.
15 Zundler S, Becker E, Spocinska M, *et al*. Hobit- and Blimp-1-driven $CD4^+$ tissue-resident memory T cells control chronic intestinal inflammation. *Nat Immunol* 2019;20:288–300.
16 Hadley GA, Higgins JMG. Integrin αEβ7: molecular features and functional significance in the immune system. *Adv Exp Med Biol* 2014;819:97–110.

17 Mueller SN, Mackay LK. Tissue-resident memory T cells: local specialists in immune defence. *Nat Rev Immunol* 2016;16:79–89.
18 Milner JJ, Goldrath AW. Transcriptional programming of tissue-resident memory CD8$^+$ T cells. *Curr Opin Immunol* 2018;51:162–9.
19 Cepek KL, Shaw SK, Parker CM, *et al*. Adhesion between epithelial cells and T lymphocytes mediated by E-cadherin and the alpha E beta 7 integrin. *Nature* 1994;372:190–3.
20 Park SL, Buzzai A, Rautela J, *et al*. Tissue-resident memory CD8$^+$ T cells promote melanoma-immune equilibrium in skin. *Nature* 2019;565:366–71.
21 Milner JJ, Toma C, Yu B, *et al*. Runx3 programs CD8$^+$ T cell residency in non-lymphoid tissues and tumours. *Nature* 2017;552:253–7.
22 Ganesan A-P, Clarke J, Wood O, *et al*. Tissue-resident memory features are linked to the magnitude of cytotoxic T cell responses in human lung cancer. *Nat Immunol* 2017;18:940–50.
23 Savas P, Virassamy B, Ye C, *et al*. Single-cell profiling of breast cancer T cells reveals a tissue-resident memory subset associated with improved prognosis. *Nat Med* 2018;24:986–93.
24 Wang B, Wu S, Zeng H, *et al*. CD103+ tumor infiltrating lymphocytes predict a favorable prognosis in urothelial cell carcinoma of the bladder. *J Urol* 2015;194:556–62.
25 Li R, Liu H, Cao Y, *et al*. Identification and validation of an immunogenic subtype of gastric cancer with abundant intratumoural CD103$^+$CD8$^+$ T cells conferring favourable prognosis. *Br J Cancer* 2020;122:1525–34.
26 Komdeur FL, Prins TM, van de Wall S, *et al*. CD103+ tumor-infiltrating lymphocytes are tumor-reactive intraepithelial CD8+ T cells associated with prognostic benefit and therapy response in cervical cancer. *Oncoimmunology* 2017;6:1–14.
27 Hu W, Sun R, Chen L, *et al*. Prognostic significance of resident CD103$^+$CD8$^+$T cells in human colorectal cancer tissues. *Acta Histochem* 2019;121:657–63.
28 Workel HH, Komdeur FL, Wouters MCA, *et al*. CD103 defines intraepithelial CD8+ PD1+ tumour-infiltrating lymphocytes of prognostic significance in endometrial adenocarcinoma. *Eur J Cancer* 2016;60:1–11.
29 Koh J, Kim S, Kim M-Y, *et al*. Prognostic implications of intratumoral CD103+ tumor-infiltrating lymphocytes in pulmonary squamous cell carcinoma. *Oncotarget* 2017;8:13762–9.
30 Djenidi F, Adam J, Goubar A, *et al*. CD8+CD103+ tumor-infiltrating lymphocytes are tumor-specific tissue-resident memory T cells and a prognostic factor for survival in lung cancer patients. *J Immunol* 2015;194:3475–86.
31 Casey KA, Fraser KA, Schenkel JM, *et al*. Antigen-Independent differentiation and maintenance of effector-like resident memory T cells in tissues. *J Immunol* 2012;188:4866–75.
32 Zhang N, Bevan MJ, Factor-β TG. Transforming growth factor-β signaling controls the formation and maintenance of gut-resident memory T cells by regulating migration and retention. *Immunity* 2013;39:687–96.
33 Chang JT, Wherry EJ, Goldrath AW. Molecular regulation of effector and memory T cell differentiation. *Nat Immunol* 2014;15:1104–15.
34 Mackay LK, Wynne-Jones E, Freestone D, *et al*. T-Box transcription factors combine with the cytokines TGF-β and IL-15 to control tissue-resident memory T cell fate. *Immunity* 2015;43:1101–11.
35 Duhen T, Duhen R, Montler R, *et al*. Co-expression of CD39 and CD103 identifies tumor-reactive CD8 T cells in human solid tumors. *Nat Commun* 2018;9:2724.
36 Franciszkiewicz K, Le Floc'h A, Jalil A, *et al*. Intratumoral induction of CD103 triggers tumor-specific CTL function and CCR5-dependent T-cell retention. *Cancer Res* 2009;69:6249–55.
37 Park SL, Gebhardt T, Mackay LK. Tissue-resident memory T cells in cancer immunosurveillance. *Trends Immunol* 2019;40:735–47.
38 Webb JR, Milne K, Watson P, *et al*. Tumor-Infiltrating lymphocytes expressing the tissue resident memory marker CD103 are associated with increased survival in high-grade serous ovarian cancer. *Clin Cancer Res* 2014;20:434–44.
39 Simoni Y, Becht E, Fehlings M, *et al*. Bystander CD8$^+$ T cells are abundant and phenotypically distinct in human tumour infiltrates. *Nature* 2018;557:575–9.
40 Jansen CS, Prokhnevska N, Master VA, *et al*. An intra-tumoral niche maintains and differentiates stem-like CD8 T cells. *Nature* 2019;576:465–70.
41 Yost KE, Satpathy AT, Wells DK, *et al*. Clonal replacement of tumor-specific T cells following PD-1 blockade. *Nat Med* 2019;25:1251–9.
42 Wang P, Huang B, Gao Y, *et al*. CD103$^+$CD8$^+$ T lymphocytes in non-small cell lung cancer are phenotypically and functionally primed to respond to PD-1 blockade. *Cell Immunol* 2018;325:48–55.
43 Corgnac S, Malenica I, Mezquita L, *et al*. CD103$^+$CD8$^+$ T_{RM} Cells Accumulate in Tumors of Anti-PD-1-Responder Lung Cancer Patients and Are Tumor-Reactive Lymphocytes Enriched with Tc17. *Cell Rep Med* 2020;1:100127.
44 Wu TD, Madireddi S, de Almeida PE, *et al*. Peripheral T cell expansion predicts tumour infiltration and clinical response. *Nature* 2020;579:274–8.
45 Mariathasan S, Turley SJ, Nickles D, *et al*. Tgfβ attenuates tumour response to PD-L1 blockade by contributing to exclusion of T cells. *Nature* 2018;554:544–8.
46 Oh DY, Kwek SS, Raju SS, *et al*. Intratumoral CD4$^+$ T cells mediate anti-tumor cytotoxicity in human bladder cancer. *Cell* 2020;181:1612–3.
47 Rosenberg JE, Hoffman-Censits J, Powles T, *et al*. Atezolizumab in patients with locally advanced and metastatic urothelial carcinoma who have progressed following treatment with platinum-based chemotherapy: a single-arm, multicentre, phase 2 trial. *Lancet* 2016;387:1909–20.
48 Powles T, Durán I, van der Heijden MS, *et al*. Atezolizumab versus chemotherapy in patients with platinum-treated locally advanced or metastatic urothelial carcinoma (IMvigor211): a multicentre, open-label, phase 3 randomised controlled trial. *Lancet* 2018;391:748–57.
49 Rittmeyer A, Barlesi F, Waterkamp D, *et al*. Atezolizumab versus docetaxel in patients with previously treated non-small-cell lung cancer (oak): a phase 3, open-label, multicentre randomised controlled trial. *Lancet* 2017;389:255–65.
50 Hegde PS, Karanikas V, Evers S. The where, the when, and the how of immune monitoring for cancer immunotherapies in the era of checkpoint inhibition. *Clin Cancer Res* 2016;22:1865–74.
51 Mackay LK, Minnich M, Kragten NAM, *et al*. Hobit and Blimp1 instruct a universal transcriptional program of tissue residency in lymphocytes. *Science* 2016;352:459–63.
52 Kavurma MM, Khachigian LM. Signaling and transcriptional control of Fas ligand gene expression. *Cell Death Differ* 2003;10:36–44.
53 Ng SS, De Labastida Rivera F, Yan J, *et al*. The NK cell granule protein NKG7 regulates cytotoxic granule exocytosis and inflammation. *Nat Immunol* 2020;21:1205–18.
54 Becht E, McInnes L, Healy J, *et al*. Dimensionality reduction for visualizing single-cell data using UMAP. *Nat Biotechnol* 2018;37:38–44.
55 Molodtsov A, Turk MJ. Tissue resident CD8 memory T cell responses in cancer and autoimmunity. *Front Immunol* 2018;9:2810.
56 Brenchley JM, Karandikar NJ, Betts MR, *et al*. Expression of CD57 defines replicative senescence and antigen-induced apoptotic death of CD8+ T cells. *Blood* 2003;101:2711–20.
57 Zhao Y, Shao Q, Peng G. Exhaustion and senescence: two crucial dysfunctional states of T cells in the tumor microenvironment. *Cell Mol Immunol* 2020;17:27–35.
58 Pardoll DM. The blockade of immune checkpoints in cancer immunotherapy. *Nat Rev Cancer* 2012;12:252–64.
59 Hoekstra ME, Bornes L, Dijkgraaf FE, *et al*. Long-distance modulation of bystander tumor cells by CD8$^+$ T cell-secreted IFNγ. *Nat Cancer* 2020;1:291–301.
60 Oja AE, Piet B, van der Zwan D, *et al*. Functional heterogeneity of CD4$^+$ tumor-infiltrating lymphocytes with a resident memory phenotype in NSCLC. *Front Immunol* 2018;9:2654.
61 Bratke K, Kuepper M, Bade B, *et al*. Differential expression of human granzymes A, B, and K in natural killer cells and during CD8+ T cell differentiation in peripheral blood. *Eur J Immunol* 2005;35:2608–16.
62 Huang M, Wang H, Hu X, *et al*. lncRNA MALAT1 binds chromatin remodeling subunit BRG1 to epigenetically promote inflammation-related hepatocellular carcinoma progression. *Oncoimmunology* 2018;8:1–14.
63 Siddiqui I, Schaeuble K, Chennupati V, *et al*. Intratumoral Tcf1$^+$PD-1$^+$CD8$^+$ T cells with stem-like properties promote tumor control in response to vaccination and checkpoint blockade immunotherapy. *Immunity* 2019;50:195–211.
64 Gherardin NA, Souter MN, Koay H-F, *et al*. Human blood MAIT cell subsets defined using MR1 tetramers. *Immunol Cell Biol* 2018;96:507–25.
65 Khan O, Giles JR, McDonald S, *et al*. TOX transcriptionally and epigenetically programs CD8$^+$ T cell exhaustion. *Nature* 2019;571:211–8.
66 Scott AC, Dündar F, Zumbo P, *et al*. TOX is a critical regulator of tumour-specific T cell differentiation. *Nature* 2019;571:270–4.
67 Guo X, Zhang Y, Zheng L, *et al*. Global characterization of T cells in non-small-cell lung cancer by single-cell sequencing. *Nat Med* 2018;24:978–85.
68 Tirosh I, Izar B, Prakadan SM, *et al*. Dissecting the multicellular ecosystem of metastatic melanoma by single-cell RNA-seq. *Science* 2016;352:189–96.

69 Li H, van der Leun AM, Yofe I, *et al*. Dysfunctional CD8 T cells form a proliferative, dynamically regulated compartment within human melanoma. *Cell* 2019;176:775–89.
70 Chen DS, Mellman I. Oncology meets immunology: the cancer-immunity cycle. *Immunity* 2013;39:1–10.
71 Blank CU, Haining WN, Held W, *et al*. Defining 'T cell exhaustion'. *Nat Rev Immunol* 2019;19:665–74.
72 Ribas A. Adaptive immune resistance: how cancer protects from immune attack. *Cancer Discov* 2015;5:915–9.
73 Philip M, Fairchild L, Sun L, *et al*. Chromatin states define tumour-specific T cell dysfunction and reprogramming. *Nature* 2017;545:452–6.
74 Pauken KE, Sammons MA, Odorizzi PM, *et al*. Epigenetic stability of exhausted T cells limits durability of reinvigoration by PD-1 blockade. *Science* 2016;354:1160–5.
75 Miller BC, Sen DR, Al Abosy R, Abosy Al R, *et al*. Subsets of exhausted $CD8^+$ T cells differentially mediate tumor control and respond to checkpoint blockade. *Nat Immunol* 2019;20:326–36.
76 Im SJ, Hashimoto M, Gerner MY, *et al*. Defining CD8+ T cells that provide the proliferative burst after PD-1 therapy. *Nature* 2016;537:417–21.
77 Clarke J, Panwar B, Madrigal A, *et al*. Single-cell transcriptomic analysis of tissue-resident memory T cells in human lung cancer. *J Exp Med* 2019;216:2128–49.
78 Xiong H, Mittman S, Rodriguez R, *et al*. Coexpression of inhibitory receptors enriches for activated and functional $CD8^+$ T cells in murine syngeneic tumor models. *Cancer Immunol Res* 2019;7:963–76.
79 O'Brien SM, Klampatsa A, Thompson JC, *et al*. Function of human tumor-infiltrating lymphocytes in early-stage non-small cell lung cancer. *Cancer Immunol Res* 2019;7:896–909.
80 Chatterjee B, Deng Y, Holler A, *et al*. Cd8+ T cells retain protective functions despite sustained inhibitory receptor expression during Epstein-Barr virus infection in vivo. *PLoS Pathog* 2019;15:e1007748.
81 Abd Hamid M, Colin-York H, Khalid-Alham N, *et al*. Self-maintaining $CD103^+$ cancer-specific T cells are highly energetic with rapid cytotoxic and effector responses. *Cancer Immunol Res* 2020;8:203–16.
82 Thommen DS, Koelzer VH, Herzig P, *et al*. A transcriptionally and functionally distinct $PD\text{-}1^+$ $CD8^+$ T cell pool with predictive potential in non-small-cell lung cancer treated with PD-1 blockade. *Nat Med* 2018;24:994–1004.
83 Romero D. B cells and TLSs facilitate a response to ICI. *Nat Rev Clin Oncol* 2020;17:195–5.
84 Smazynski J, Webb JR. Resident memory-like tumor-infiltrating lymphocytes (TIL_{RM}): latest players in the immuno-oncology repertoire. *Front Immunol* 2018;9:1741.
85 Fonseca R, Beura LK, Quarnstrom CF, *et al*. Developmental plasticity allows outside-in immune responses by resident memory T cells. *Nat Immunol* 2020;21:412–21.
86 Lawrence M, Huber W, Pagès H, *et al*. Software for computing and annotating genomic ranges. *PLoS Comput Biol* 2013;9:e1003118–10.
87 Ritchie ME, Phipson B, Wu D, *et al*. limma powers differential expression analyses for RNA-sequencing and microarray studies. *Nucleic Acids Res* 2015;43:e47.
88 Jassal B, Matthews L, Viteri G, *et al*. The reactome pathway knowledgebase. *Nucleic Acids Res* 2020;48:D498–503.
89 Yu G, He Q-Y. ReactomePA: an R/Bioconductor package for reactome pathway analysis and visualization. *Mol Biosyst* 2016;12:477–9.
90 Zheng GXY, Terry JM, Belgrader P, *et al*. Massively parallel digital transcriptional profiling of single cells. *Nat Commun* 2017;8:14049–12.
91 Stuart T, Butler A, Hoffman P, *et al*. Comprehensive integration of single-cell data. *Cell* 2019;177:1888–902.
92 Aran D, Looney AP, Liu L, *et al*. Reference-based analysis of lung single-cell sequencing reveals a transitional profibrotic macrophage. *Nat Immunol* 2019;20:163–72.
93 Del Carratore F, Jankevics A, Eisinga R, *et al*. RankProd 2.0: a refactored Bioconductor package for detecting differentially expressed features in molecular profiling datasets. *Bioinformatics* 2017;33:2774–5.
94 Diedenhofen B, Musch J. cocor: a comprehensive solution for the statistical comparison of correlations. *PLoS One* 2015;10:e0121945.
95 Chao A, Gotelli NJ, Hsieh TC, *et al*. Rarefaction and extrapolation with Hill numbers: a framework for sampling and estimation in species diversity studies. *Ecol Monogr* 2014;84:45–67.
96 Zeileis A, Fisher JC, Hornik K. colorspace: a toolbox for manipulating and assessing colors and Palettes. *arXiv*2019;06490:1903:1–45.
97 Barter RL, Yu B. Superheat: an R package for creating beautiful and extendable heatmaps for visualizing complex data. *J Comput Graph Stat* 2018;27:910–22.